Chemical Engineering Journal 215-216 (2013) 550–560

Contents lists available at SciVerse ScienceDirect

Chemical Engineering Journal

journal homepage: www.elsevier.com/locate/cej

Modeling of ethane pyrolysis process: A study on effects of steam and carbon dioxide on ethylene and hydrogen productions

M.S. Shokrollahi Yancheshmeh [a], S. Seifzadeh Haghighi [a], M.R. Gholipour [a], O. Dehghani [a], M.R. Rahimpour [a,b,*], S. Raeissi [a]

[a] Department of Chemical Engineering, School of Chemical and Petroleum Engineering, Shiraz University, Shiraz 71345, Iran
[b] Gas Center of Excellence, Shiraz University, Shiraz 71345, Iran

HIGHLIGHTS

- A mathematical model was developed to simulate thermal cracking of ethane.
- A comparison between mathematical and plant data show an acceptable agreement.
- The mathematical model was run with carbon dioxide instead of steam.
- Using carbon dioxide can enhance production yields and decrease coke deposition.
- Using CO_2 increases the run length of reactor as twice as the conventional one.

GRAPHICAL ABSTRACT

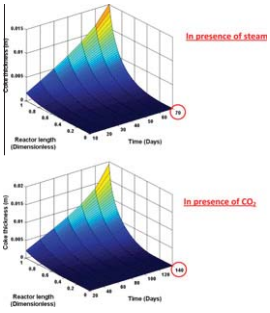

ARTICLE INFO

Article history:
Received 4 August 2012
Received in revised form 4 October 2012
Accepted 9 October 2012
Available online 12 November 2012

Keywords:
Thermal cracking
Coke formation
Ethane cracking in presence of steam
Ethane cracking in presence of carbon dioxide
Reactor modeling
Hydrogen production

ABSTRACT

In present work, ethylene and hydrogen production is investigated through thermal cracking of ethane in domestic petrochemical plant. In the thermal cracking process, a mixture of ethane and steam is introduced into radiant tubes located vertically in a furnace. The use of steam is mainly due to the partial removal of coke which has undesirable effects on the process. The coke deposition along the tubes causes high pressure drops and also reduction in production yield. In this study, the ethane thermal cracking process of this company is modeled and solved numerically. A comparison between model results and experimental data shows that the model can predict the process accurately. In addition, the effects of using carbon dioxide instead of steam are investigated on coke deposition. According to the results of two cases, the thermal cracking process in presence of CO_2 is superior to the conventional process because of higher ethylene and hydrogen productions and less coke thickness. The simulation results reveal that the run length of the reactor in presence of CO_2 becomes as twice as the one in presence of steam.

1. Introduction

1.1. Hydrogen

In recent years, the depletion of energy resources such as fossil fuels forces researchers to pursue an appropriate solution for this problem which should be more environmentally friendly. It is generally accepted that hydrogen is a good alternative for

* Corresponding author at: Department of Chemical Engineering, School of Chemical and Petroleum Engineering, Shiraz University, Shiraz 71345, Iran. Tel.: +98 711 2303071; fax: +98 711 6287294.
E-mail address: rahimpor@shirazu.ac.ir (M.R. Rahimpour).

1385-8947/$ - see front matter © 2012 Elsevier B.V. All rights reserved.
http://dx.doi.org/10.1016/j.cej.2012.10.078

Nomenclature

C	concentration of coke (mole m^{-3})
C_p	heat capacity (J $mole^{-1}$ K^{-1})
d_t	coil diameter (m)
F_i	molar flow rate of component I (mole s^{-1})
Fr	friction factor
G	total mass flow rate (kg m^{-2} s^{-1})
k_i	rate coefficient of reaction i (s^{-1} or l $mole^{-1}$ s^{-1})
M_c	coke molecular weight (kg $mole^{-1}$)
M_m	average molecular weight (kg $mole^{-1}$)
P_t	total pressure (Pa)
Q	heat flux (W m^{-2})
r_c	rate of coking (mole m^{-2} s^{-1})
r_i	rate of reaction i (mole m^{-2} s^{-1})
R	universal gas constant (J $mole^{-1}$ K^{-1})
R_b	radius of the tube bend (m)
Re	Reynolds number
s_{ij}	stoichiometric coefficient of component jth in ith reaction
T	Temperature (K)
t	time (s)
t_c	coke thickness (m)
z	axial reactor coordinate (m)

Greek letters

ΔH	heat of reaction (J $K\ mol^{-1}$)
η	conversion factor (atm Pa^{-1})
ξ	parameter of tube bend
Λ	angel of bend
α	coking factor
ρ_c	coke specific gravity (kg m^{-3})

conventional fuels [1]. Hydrogen will be a key contribution to sustainable development, because in near future it will be produced in virtually unlimited quantities using various methods [2]. Due to the increased demand for hydrogen in various processes such as petroleum refining and petrochemical industries, production of hydrogen has noticeable importance [3]. The most worldwide demands for hydrogen can be categorized as follow: ammonia production (49%), petroleum refining (37%), methanol production (8%), and other smaller-volume usages (6%) [2].

Hydrogen can be generated by various procedures such as electrolysis of water, biomass pyrolysis, and natural gas reforming. Moreover, catalytic steam reforming of natural gas and other hydrocarbons is the main way to produce hydrogen [4,5]. However, some researchers suggested that thermal cracking process of ethane or other hydrocarbons such as naphtha and crude oil can be used to generate hydrogen. There is no doubt that one of the by-products of pyrolysis processes is hydrogen, which is produced nearly as many as the main products. As a result, these methods are suggested as other sources of hydrogen energy [6].

1.2. Ethylene

Ethylene is one of the fundamental elements of petrochemical industry used as a main feed stock for the production of plastics, particularly polyethylene. Ethylene is known as a base component for many petrochemical industries because of its low cost and high purity. In addition, ethylene reacts with other low cost components such as oxygen and water and produces useful chemicals.

Ethylene production had a dramatic growth in the late 20th century from 29 to 180 billion lb [7]. Consequently, it is known that even a small improvement in ethylene processes can lead to remarkable profits for the petrochemical industries [8,9]. Currently, the most important methods of ethylene production are thermal cracking of alkanes such as ethane, propane, butane, naphtha and gas oil [10–12]. This method is also used for ethylene production in Jam Petrochemical Company which is the largest olefin plant in the world. This company produces 1,324,000 tons of ethylene per year with both gas and liquid crackers using ethane and naphtha as a feedstock, respectively.

1.3. Thermal cracking

Hydrocarbon thermal cracking process is the major route for olefin production. In this process, a mixture of steam and hydrocarbons including ethane, propane, butane, isobutane, naphtha, and gas oil is introduced into furnaces in order to produce olefins. The main parameters affecting the product distribution are feed composition, reactor gas temperature and steam ratio. Over the last several decades, many attempts had been done on the modeling of thermal cracking process for various hydrocarbons. Lee and Aitani investigated the influence of feed composition for ethylene production [4]. Keyvanloo et al. studied the effects of steam ratio, temperature and residence time on the products yields in steam cracking process of naphtha [13]. Belohlav et al. presented a model to describe thermal cracking of ethane, petroleum gases, and primary naphtha [14].

Fundamental free radical reactions of pyrolysis process were explained entirely by Poutsma [15]. Moreover, Sundaram and Froment suggested a free radical reaction network that was used to model the pyrolysis of ethane, propane, *n*-butane, *i*-butane, and simple mixtures of them [16]. Ghassabzadeh et al. examined the production of ethylene and propylene by kerosene thermal cracking in an experimental setup. They used some simplification assumptions to report an appropriate kinetic model that predicted product yields accurately [17]. Effects of temperature, residence time and steam ratio on main products in gas–oil thermal cracking processes were studied by Depeyre et al. They developed a model for product distributions on the basis of radical mechanism [18]. Towfighi et al. suggested a reaction network model to simulate LPG cracking plants [19]. In addition, other researchers presented some mechanistic models for the atmospheric gas–oil cracking process based on experimental data [20,21].

1.4. Coking

Thermal cracking of hydrocarbons always accompanies carbonaceous deposition. This phenomenon depends on different factors such as sulfur and aromatic content of feedstock, partial pressure of hydrocarbons and building materials of the reactor. Coke formation has serious consequences on the pyrolysis process and the most undesirable one is the reduction of heat flux to the reactor. To keep the heat transfer in the desired level, the skin temperature should be raised gradually while it has some limitations. It is clear that coil metallurgy is the main limitation for tube wall temperature rise. Furthermore, the increase of skin temperature leads to a high coke formation rate and declines the efficiency of radiation section. Besides, cross section reduction of the coils, which is caused by coke deposition, increases the pressure drop along tubes and in the severe situations it clogs up the reactor. Reduction in

Table 1
Outlet compositions of liquid furnaces.

Component	Mass (dry%)	Mass (wet%)	Flow (ton/h)
Water	0.00	33.33	22.182
Hydrogen	1.12	0.75	0.498
Methane	19.93	13.29	8.843
Carbon monoxide	0.13	0.09	0.058
Carbon dioxide	0.01	0.01	0.005
Sum C_0/C_1's	21.20	47.47	31.587
Acetylene	0.86	0.57	0.379
Ethylene	***34.11***	**22.74**	**15.134**
Ethane	3.44	2.29	1.525
Sum C_2's	38.40	25.60	17.038
C_3H_4's	1.19	0.79	0.528
Propylene	15.39	10.26	6.828
Propane	0.85	0.57	0.378
Sum C_3's	17.43	11.62	7.734
Vinyl acetylene	0.12	0.08	0.054
Butadiene	4.66	3.11	2.069
Butenes	4.01	2.67	1.778
Butanes	1.55	1.03	0.686
Sum C_4's	10.34	6.89	4.587
Sum C_5's	2.40	1.60	1.064
Benzene	5.18	3.46	2.30
C_6 Non-aromatics	0.50	0.33	0.223
Sum C_6's	5.69	3.79	2.523
Toluene	1.57	1.04	0.695
C_7 Non-aromatics	0.10	0.07	0.044
Sum C_7's	1.67	1.11	0.739
Xylenes	0.26	0.17	0.115
Ethyl benzene	0.02	0.02	0.010
Styrene	0.57	0.38	0.251
C_8 Non-aromatics	0.00	0.00	0.002
Sum C_8's	0.85	0.57	0.379
Sum C_9's	0.25	0.17	0.112
Sum C_{10+}'s	1.77	1.18	0.785
Total	100.00	100.00	66548

Table 2
Outlet compositions of gas furnaces.

Component	Mass (dry%)	Mass (wet%)	Flow (ton/h)
Water	0.00	23.08	11.916
Hydrogen	3.89	2.99	1.546
Methane	4.75	3.65	1.886
Carbon monoxide	0.04	0.03	0.018
Carbon dioxide	0.01	0.01	0.005
Sum C_0/C_1's	8.70	29.77	15.370
Acetylene	0.34	0.26	0.136
Ethylene	***50.75***	**39.03**	**20.156**
Ethane	35.55	27.35	14.120
Sum C_2's	86.64	66.64	34.411
C_3H_4's	0.02	0.02	0.009
Propylene	1.12	0.86	0.443
Propane	0.20	0.15	0.080
Sum C_3's	1.34	1.03	0.532
Vinyl acetylene	0.03	0.03	0.014
Butadiene	1.20	0.92	0.478
Butenes	0.16	0.12	0.063
Butanes	0.37	0.29	0.149
Sum C_4's	1.77	1.36	0.703
Sum C_5's	0.40	0.31	0.160
Benzene	0.77	0.59	0.304
C_6 Non-aromatics	0.03	0.02	0.011
Sum C_6's	0.79	0.61	0.315
Toluene	0.10	0.07	0.038
C_7 Non-aromatics	0.01	0.00	0.002
Sum C_7's	0.10	0.08	0.040
Xylenes	0.00	0.00	0.001
Ethyl benzene	0.00	0.00	0.001
Styrene	0.08	0.06	0.031
C_8 Non-aromatics	0.00	0.00	0.000
Sum C_8's	0.08	0.06	0.033
Sum C_9's	0.01	0.01	0.004
Sum C_{10+}'s	0.17	0.13	0.066
Total	100.00	100.00	51635

ethylene selectivity and increase in maintenance and utility costs are the other results of coke formation phenomenon [22–25].

The mentioned problems force the plant operators to shut down the unit for decoking process. A typical run length of the cracking reactor is 30–90 days that depends on the type of reactor, feedstock and operating conditions. The decoking process is carried out by burning the coke using a mixture of air and steam. As a result, coils life time shortens gradually due to the constant thermal cycling. Therefore, it is vital to minimize the amount of coke deposited on the tube walls [22–25].

Investigations proved that either of reactants and/or products can form coke. Virk et al. claimed that aromatic substances condensation is a reason of coke formation [26]. Froment et al. pointed out that propylene is the main coke precursor in the pyrolysis of propane while butadiene and aromatics are the main reasons of coke deposition in the ethane thermal cracking process. They also believed that a first order kinetic could predict the rate of coke formation precisely based on the concentration of a number of products such as olefins, diolefins, butene, butadiene, C_{5+}, and aromatics [27]. Furthermore, some scientists developed a correlation for coke formation rates as a function of run time [28]. Kumar and Kunzru introduced aromatics as coke precursors in thermal cracking of naphtha, whereas other researchers showed that both ethylene and propylene components play a noticeable role as coke precursors in the thermal cracking process. They also argued that the function of ethylene is more effective than propylene [29–31].

In this work, the simulation of thermal cracking reactor of domestic petrochemical company is conducted and the results are compared with the industrial data. After model validation, CO_2 is used instead of steam and the influences of this change are investigated on the product yield and coke thickness along the reactor.

2. Process description

As mentioned above, both gas and liquid furnaces are used worldwide in order to produce olefins. Tables 1 and 2 provide information about the products of liquid and gas furnaces from domestic petrochemical company, respectively. It is noticeable that gas furnace produces 1.5 times more ethylene than liquid furnace [32].

Ethane is one of the best feedstock for thermal cracking process because of its high ethylene selectivity in comparison with other heavier paraffin. Moreover, pyrolysis of ethane is comparatively simple and cheaper than other hydrocarbon. In domestic petrochemical company, a mixture of ethane and steam goes through two passes in gas furnaces. Table 3 shows flow rates of ethane and steam in each pass in a typical gas furnace during a run length of reactor.

The ethane cracking furnace is composed of convection and radiation sections as depicted in Fig. 1. The feed is introduced into the convection section at 121 °C and 5.9 bars. This stream is diluted with steam (0.3 kg steam/kg ethane) at 175 °C and 5.7 bars. Then, this mixture is preheated to around 500–800 °C by using hot stack gas. After that it goes into the radiation section, where ethane molecules break up to produce ethylene, propylene, butadiene, methane and other products. This procedure takes place in radiant tubes that are located vertically in a rectangular furnace at 700–900 °C

Table 3
Flow rate of ethane and dilution steam during a run length of reactor.

Time (day)	Pass 1		Pass 2	
	Flow rate of ethane (kg/h)	Flow rate of steam (kg/h)	Flow rate of ethane (kg/h)	Flow rate of steam (kg/h)
2	19995	6195	20000	6206
4	20004	6249	19979	6211
6	19987	6214	20006	6206
8	19956	6212	19961	6217
10	19994	6159	19994	6208
12	19929	6114	20023	6204
14	20037	6199	20029	6176
16	19984	6182	19984	6198
18	18403	6540	18177	6572
20	17407	6745	17482	6808
22	14064	8762	13967	8790
24	14088	8756	14014	8756
26	14021	8728	13986	8773
28	14088	8743	13962	8722
30	14034	8754	14023	8778
32	13804	8705	13977	8914
34	13910	8749	14009	8795
36	13957	8966	14008	8894
38	14011	8810	14007	8862
40	14045	8770	13996	8798
42	13989	8763	14029	8714
44	13991	8798	13990	8784
46	17275	7057	16966	7116
48	19833	5879	19971	6021
50	19736	5801	19955	6030
52	19968	5912	20010	6010
54	20128	5958	20041	6012
56	20075	5980	20007	6025
58	20159	6066	19988	6038
60	20163	6139	20097	6103

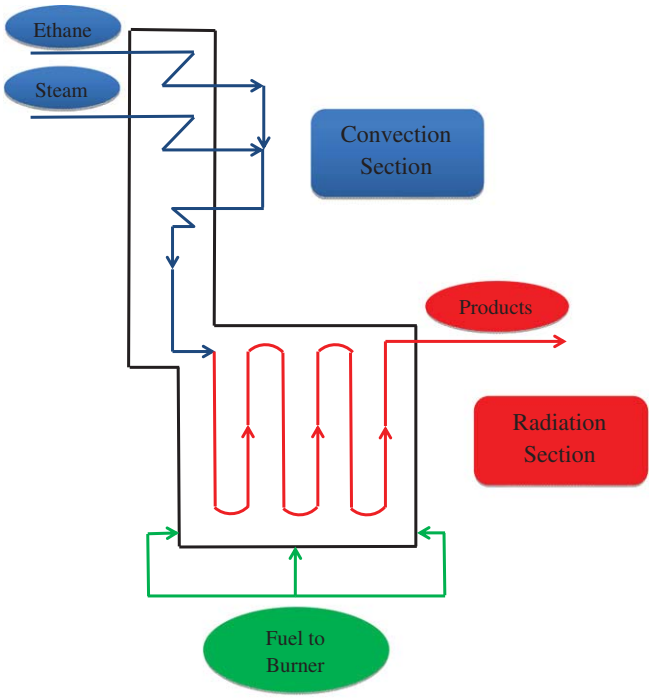

Fig. 1. Process diagram furnace in thermal cracking of ethane.

[33]. Forty side burners and 40 bottom burners provide the required heat to maintain the reactor temperature at this range. In this process, temperature role is of paramount importance for output concentrations and so the coil outlet temperature (COT) of these furnaces should be kept constant at 800 °C. Table 4 provides some information about coil outlet temperatures (COTs) and pressures. After that, products at 775–885 °C leave the furnaces and cool down quickly in the transfer line exchanger (TLE) in order to prevent other side reactions. Finally, the products are compressed and sent for other separation steps as it is shown in Fig. 2. Table 5 shows the specific properties and operating conditions of the cracking coils in domestic plant.

Table 4
Coil outlet temperature and pressure.

Time (day)	Pass 1		Pass 2	
	Coil outlet temperature (°C)	Coil outlet pressure (bar)	Coil outlet temperature (°C)	Coil outlet pressure (bar)
2	623.3	3.337	625.5	3.247
4	623.4	3.382	626.9	3.252
6	626.4	3.332	629.4	3.257
8	627.5	3.353	630.3	3.270
10	625.1	3.328	628.2	3.255
12	628.3	3.342	631.7	3.269
14	621.8	3.333	625.7	3.261
16	630.4	3.351	633.2	3.251
18	625.9	3.194	631.2	3.073
20	633.3	3.061	636.2	2.995
22	618.8	2.967	623.9	2.878
24	622.9	2.930	626.9	2.834
26	620.6	2.932	625.0	2.855
28	621.2	2.930	625.1	2.843
30	621.1	2.901	624.3	2.840
32	621.1	2.863	624.3	2.865
34	616.0	2.867	622.1	2.825
36	619.4	2.931	622.6	2.857
38	605.2	2.860	608.0	2.808
40	582.3	2.807	586.3	2.758
42	572.2	2.766	579.9	2.718
44	570.7	2.811	577.1	2.773
46	580.0	2.965	583.6	2.893
48	615.4	3.197	618.7	3.185
50	623.9	3.195	624.6	3.205
52	616.2	3.235	617.5	3.211
54	620.9	3.211	624.3	3.110
56	623.4	3.225	627.2	3.141
58	618.2	3.209	623.1	3.131
60	619.3	3.211	623.4	3.147

As it was mentioned above, steam is added to the feed in order to reduce the partial pressure of high-molecular mass aromatics. It also lowers the number of condensation reactions and contributes to the partial removal of coke in the tubes. Choudhary et al. stated that carbon dioxide is a mild oxidant which can play the role of steam in pyrolysis process [34]. In the following model, steam is replaced by CO_2 and its influences on the product distributions and coke removal are investigated. The model was run with the same operating conditions relative to the conventional one except that 2 kg CO_2/kg ethane is added instead of steam.

3. Kinetic model

Several molecular reaction schemes had been proposed for pyrolysis of ethane. In this paper, the Forment's molecular scheme is utilized [35]. According to this model, the following reactions are considered:

$$C_2H_6 \leftrightarrow C_2H_4 + H_2 \quad \Delta H = 136,330,000 \ (\mathrm{J/K\ mol}) \tag{1}$$

$$2C_2H_6 \rightarrow C_3H_8 + CH_4 \quad \Delta H = -11,560,000 \ (\mathrm{J/K\ mol}) \tag{2}$$

$$C_3H_8 \rightarrow C_3H_6 + H_2 \quad \Delta H = 124,910,000 \ (\mathrm{J/K\ mol}) \tag{3}$$

$$C_3H_8 \rightarrow C_2H_4 + CH_4 \quad \Delta H = 82,670,000 \ (\mathrm{J/K\ mol}) \tag{4}$$

$$C_3H_8 \leftrightarrow C_2H_2 + CH_4 \quad \Delta H = 133,450,000 \ (\mathrm{J/K\ mol}) \tag{5}$$

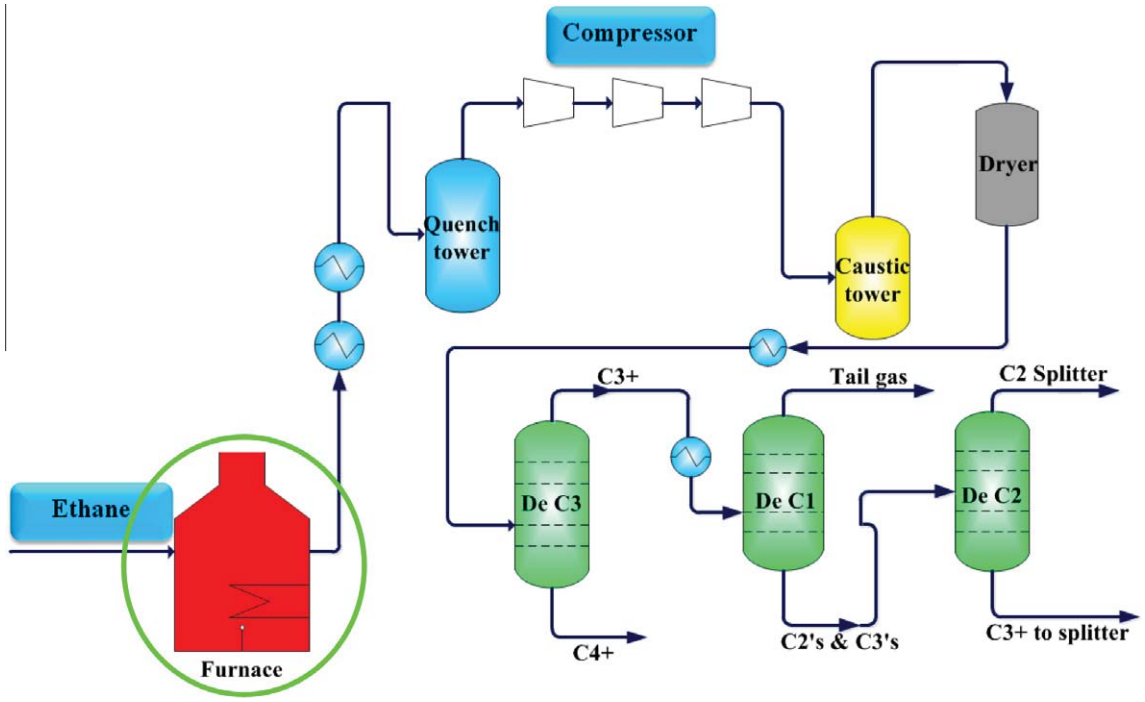

Fig. 2. A typical cracking plants and separation utilities.

Table 5
Characteristics of cracking reactor of Jam Petrochemical Industry for ethane cracking.

Reactor characteristics	
Length	78 m
Inner diameter	0.1 m
Wall thickness	0.008 m
Feed and operating conditions	
Ethane flow rate	40047 kg/h
Steam flow rate	12014 kg/h
Inlet temperature	695
Outlet temperature	845
Inlet pressure	3.09 bar
Outlet pressure	2.12 bar
Coke properties	
Specific gravity of coke	1600 kg/m^3
Thermal conductivity of coke	5.5 W/m K

Table 6
Arrhenius parameters for thermal cracking of ethane.

Rate coefficient	A (s^{-1} or l $mole^{-1}$ s^{-1})	E (J/mole)
k_1	4.65E+13	2.73E+05
k_2	3.85E+11	2.73E+05
k_3	5.89E+10	2.15E+05
k_4	4.69E+10	2.12E+05
k_5	6.81E+08	1.54E+05
k_6	1.03E+09	1.73E+05
k_7	6.37E+23	5.30E+05
k_8	7.08E+10	2.53E+05
k_{17}	5.00E+14	2.24E+05
k_{18}	2.77E+09	1.16E+05
k_{19}	5.61E+18	2.74E+05
k_{23}	5.09E+04	2.38E+05
k_{24}	1.12E+08	2.45E+05

$$C_2H_2 + C_2H_4 \rightarrow C_4H_6 \quad \Delta H = -171,470,000 \text{ (J/Kmol)} \tag{6}$$

$$2C_2H_6 \rightarrow C_2H_4 + 2CH_4 \quad \Delta H = 71,102,000 \text{ (J/K mol)} \tag{7}$$

Table 7
Equilibrium constants based on concentration.

Temperature (°C)	775	800	825
K_{c1}	8.90E−03	1.28E−02	1.80E−02
K_{c5}	9.85E−03	1.38E−02	1.89E−02

$$C_2H_6 + C_2H_4 \rightarrow C_3H_6 + CH_4 \quad \Delta H = -22,980,000 \text{ (J/K mol)} \tag{8}$$

The rate equations for the above reactions are given as follow [35]:

$$r_1 = k_1\left[\frac{F_{C_2H_6}}{F_t}\left(\frac{P_t}{RT}\right) - \frac{F_{C_2H_4}F_{H_2}}{F_t^2 Kc_1}\left(\frac{P_t}{RT}\right)^2\right] \tag{9}$$

$$r_2 = k_2\left[\frac{F_{C_2H_6}}{F_t}\left(\frac{P_t}{RT}\right)\right] \tag{10}$$

$$r_3 = k_3\left[\frac{F_{C_3H_8}}{F_t}\left(\frac{P_t}{RT}\right)\right] \tag{11}$$

$$r_4 = k_4\left[\frac{F_{C_3H_8}}{F_t}\left(\frac{P_t}{RT}\right)\right] \tag{12}$$

$$r_5 = k_5\left[\frac{F_{C_3H_6}}{F_t}\left(\frac{P_t}{RT}\right) - \frac{F_{C_2H_2}F_{CH_4}}{F_t^2 Kc_5}\left(\frac{P_t}{RT}\right)^2\right] \tag{13}$$

$$r_6 = k_6\left[\frac{F_{C_2H_2}F_{C_2H_4}}{F_t^2}\left(\frac{P_t}{RT}\right)^2\right] \tag{14}$$

$$r_7 = k_7\left[\frac{F_{C_2H_6}}{F_t}\left(\frac{P_t}{RT}\right)\right] \tag{15}$$

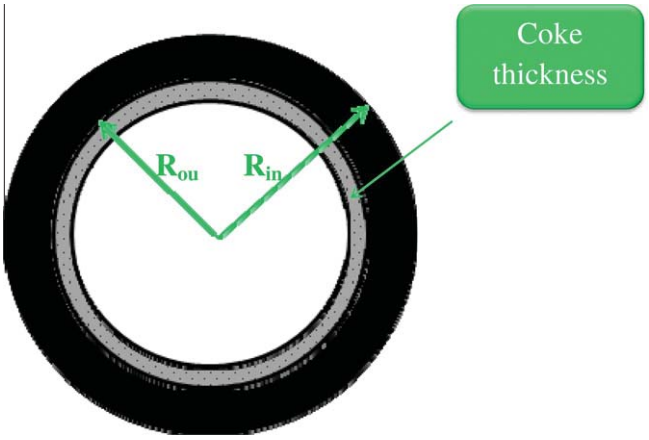

Fig. 3. Cross section of a cracking coil.

$$r_8 = k_8\left[\frac{F_{C_2H_6}F_{C_2H_4}}{F_t^2}\left(\frac{P_t}{RT}\right)^2\right] \quad (16)$$

In this article ethylene, propylene and 1,3-butadiene are also considered as the coke precursors:

$$C_2H_4 \rightarrow \text{coke} \quad (17)$$

$$C_3H_6 \rightarrow \text{coke} \quad (18)$$

$$C_4H_6 \rightarrow \text{coke} \quad (19)$$

The rate equations for these reactions are given below [31]:

$$r_{17} = k_{17}\left[\left(\frac{F_{C_2H_4}P_t}{F_tRT}\right)^{1.34}\right] \quad (20)$$

$$r_{18} = k_{18}\left[\left(\frac{F_{C_3H_6}P_t}{F_tRT}\right)^{1.34}\right] \quad (21)$$

$$r_{19} = k_{19}\left[\left(\frac{F_{C_4H_6}P_t}{F_tRT}\right)^{1.37}\right] \quad (22)$$

Partial removal of coke reactions are explained by Eqs. (23) and (24):

$$C + H_2O \rightarrow CO + H_2 \quad \Delta H = 131,000,000\ (\text{J/Kmol}) \quad (23)$$

$$C + CO_2 \rightarrow 2CO \quad \Delta H = 172,459,000\ (\text{J/Kmol}) \quad (24)$$

While the related rate equations for these reactions are:

$$r_{23} = k_{23}\left[\frac{F_{H_2O}P_t}{F_t}\right] \quad (25)$$

$$r_{24} = k_{24}\left[\left(\frac{F_{CO_2}P_t}{F_t}\right)^{0.31}\right] \quad (26)$$

The kinetic constants of above equations are tabulated in Tables 6 and 7.

4. Mathematical modeling

The cross section of the cracking coils is shown in Fig. 3. In the present study, a one dimensional model was considered and a set of equations consist of mass, energy and momentum balances were solved numerically. To simplify the mathematical model these assumptions were applied:

1. Plug flow pattern is employed.
2. The gas mixture is considered as an ideal gas.
3. Axial dispersions of mass and heat are negligible.
4. Radial concentration gradients are neglected.
5. Hydrodynamic or thermal entrance region effects are insignificant.
6. The case is investigated as a quasi-steady state in order to simulate coke deposition rate.

With the above assumptions, the governing equations are derived as follow [12]:

$$\frac{dF_j}{dz} = \left(\sum_i s_{ij}r_{ri}\right)\frac{\pi d_t^2}{4} \quad (27)$$

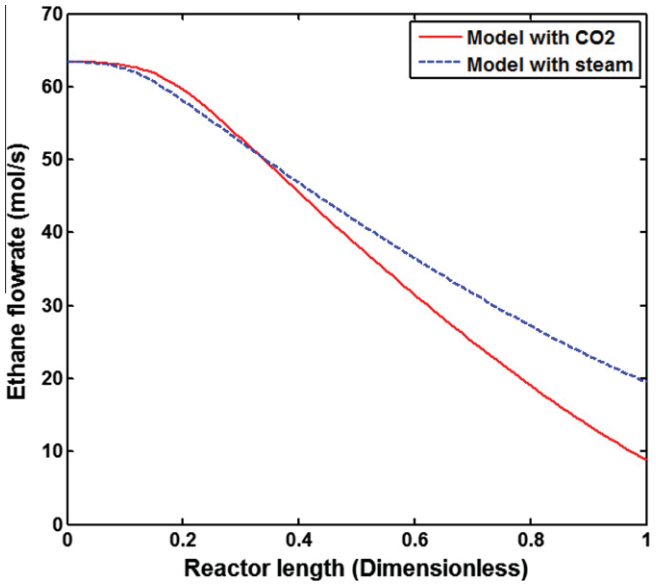

Fig. 4. The molar flow rate of ethane along the length of cracking coils.

Table 8
Comparison of modeling results with domestic petrochemical plant data.

	Plant data	Modeling results five reactions	Modeling results eight reactions	Percentage error five reactions	Percentage error eight reactions
Ethane	20.6034	20.0725	19.5322	2.576759176	5.199141889
Ethylene	34.5602	36.3475	35.8682	5.17155572	3.78470032
Hydrogen	37.3611	40.3307	39.6565	7.948374111	6.143823388
Methane	5.8102	4.6765	6.3044	19.5122371	8.5057313
Propylene	0.5081	0.3438	0.4916	32.3361543	3.247392246
Propane	0.0842	0.121	0.0864	43.70546318	2.612826603
Acetylene	0.2653	0.3777	0.2832	42.36713155	6.747078779
1,3-Butadiene	0.4424	0.687	0.4685	55.28933092	5.899638336
Temperature	1120	1164.2	1150.3	4.113754248	2.87068503

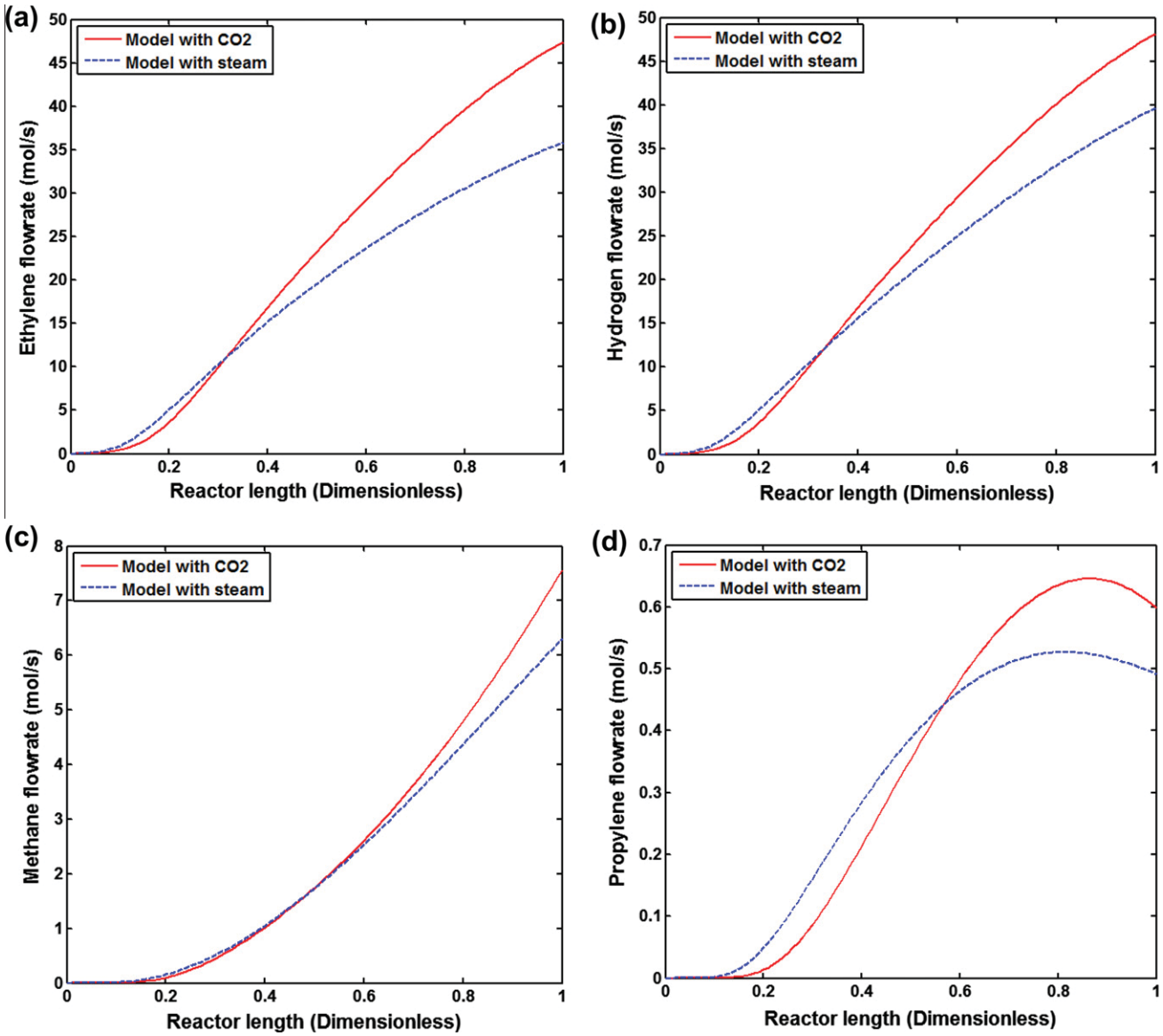

Fig. 5. The molar flow rate of (a) ethylene, (b) hydrogen, (c) methane and (d) propylene along the length of cracking coils.

$$\sum_j F_j c_{pj} \frac{dT}{dz} \equiv Q(z)\pi d_t + \frac{\pi d_t^2}{4} \sum_i r_{ri}(-\Delta H)_i \tag{28}$$

$$\left(\frac{1}{M_m P_t} - \frac{P_t}{\eta G^2 RT}\right)\frac{dP_t}{dz} = \frac{d}{dz}\left(\frac{1}{M_m}\right) + \frac{1}{M_m}\left(\frac{1}{T}\frac{dT}{dz} + Fr\right) \tag{29}$$

The friction factor for the straight parts of the cracking coils and the tube bends are given in Eqs. (30) and (31), respectively:

$$Fr = 0.092\frac{\mathrm{Re}^{-0.2}}{d_t} \tag{30}$$

$$Fr = 0.092\frac{\mathrm{Re}^{-0.2}}{d_t} + \frac{\zeta}{\pi R_b} \tag{31}$$

The parameter of tube bend (ζ) is expressed as follows:

$$\zeta = \left(0.7 + 0.35\frac{\Lambda}{90^\circ}\right)\left(0.051 + 0.19\frac{d_t}{R_b}\right) \tag{32}$$

The rate of coke formation can be calculated from the following equation:

$$\frac{\partial C}{\partial t} = (d_t - 2t_c)\frac{\alpha M_c r_c}{4\rho_c} \tag{33}$$

5. Numerical solution

Mass, energy and momentum balance equations form a set of ordinary differential equations (ODEs) that are coupled with nonlinear algebraic equations of kinetic model and auxiliary correlations. To convert this set of ODEs to nonlinear algebraic equations, backward finite difference approximation is applied. The cracking coil length is divided into 100 separate sections and the set of equations are solved for all sections simultaneously.

6. Model validation

Sundaram and Froment proposed three different kinetic mechanisms for ethane pyrolysis [22,35]. They believed that a model

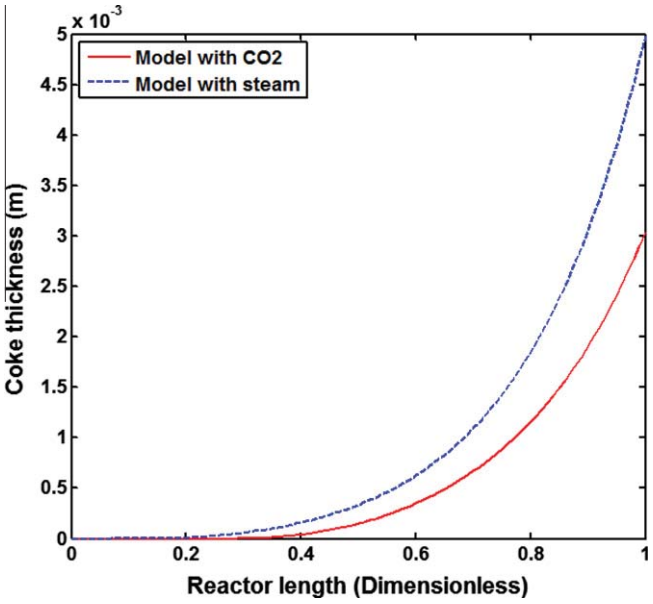

Fig. 6. The coke thickness along the length of cracking coils.

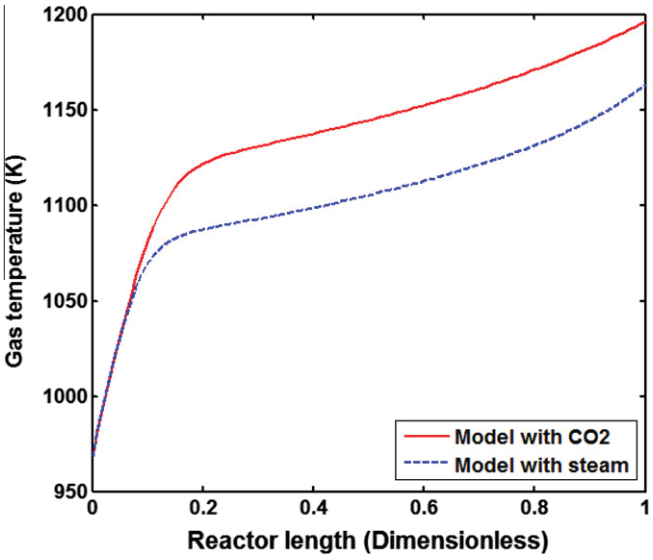

Fig. 7. The gas temperature along the length of cracking coils.

type of 5-reaction system (reactions (1), (2), (5), (6), and (8)) could predict experimental data more accurately than the two other models. However, a novel 8-reaction system, which is used in this survey, can predict plant data more precisely. Table 8 compares the results of these two models with plant data. As it is obvious, the proposed kinetic model in this study is more accurate than the 5-reaction system.

7. Results and discussions

In this section, the behaviors of the cracking coils in presence of steam and CO_2 are discussed. Furthermore, the effects of these two diluents on the ethane conversion, ethylene and hydrogen yields, coke thickness and temperature profiles along the reactor are investigated during the process.

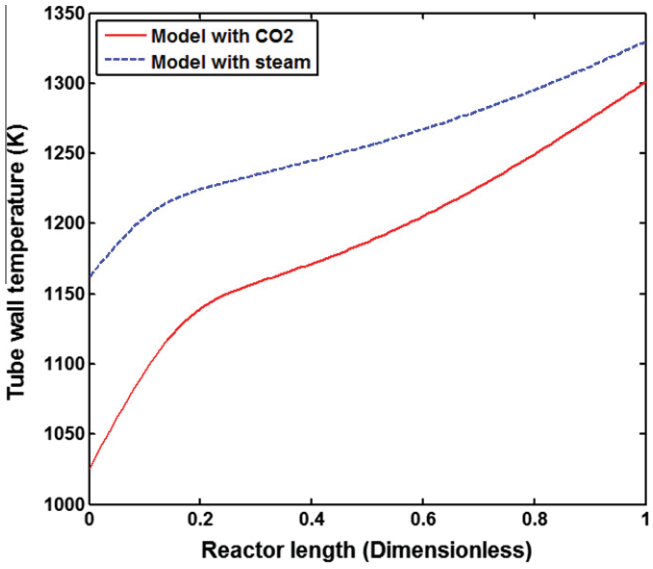

Fig. 8. The tube wall temperature along the length of cracking coils.

Fig. 4 shows the ethane flow rate along the reactor. As it can be seen, the flow rate of ethane in the entrance of the reactor for both diluents are the same while they reduce to 19.53 and 11.34 $(\frac{mol}{s})$ in presence of steam and CO_2, respectively. The main reason for much ethane conversion in presence of carbon dioxide is that ethane activates with this chemical at high temperatures which increases the rate of C–C bond cleavage. Moreover, the CO_2 usage leads to higher heat transfer to the coils due to much less coke formation in the reactor. As a result, the gas temperature increases significantly which is desirable for thermal cracking reactions. It is noticeable that the difference between ethane flow rates is negligible along 0.3 m of the cracking coils because of coke precursors' formation rates. In this length of reactor, the coke precursors (ethylene, propylene and 1,3-butadiene) are not being produced considerably and so there is no coke deposition. In contrast, the concentrations of coke precursors are high enough in order to coke formation reactions occur and as a result the effect of CO_2 and steam can be seen in the rest of reactor length.

Fig. 5a–d illustrates the flow rates of the main products of ethane pyrolysis in presence of steam and CO_2 along the length of cracking coils. According to these figures, ethylene production in presence of CO_2 increases by 9.7067 $(\frac{mol}{s})$ more than one in presence of steam. It is noticeable that this process produces hydrogen nearly as much as ethylene and so CO_2 can improve hydrogen yield as shown in Fig. 5b. Obviously, hydrogen flow rate in conventional system reaches just under 40 $(\frac{mol}{s})$, but this quantity for the novel system is more than 48 $(\frac{mol}{s})$. In addition, other products such as methane and propylene in presence of CO_2 are generated more than conventional system. These high growths in production yields are owing to more ethane conversion. As mentioned above, CO_2 cannot react with ethane at thermal cracking temperature, but it is believed that CO_2 presence causes ethane to activate more [34].

Coke thickness after 30 working days along the reactor is shown in Fig. 6. It is witnessed that coke formation in presence of CO_2 has a dramatic decline and so the coke thickness reduces about 40% relative to the conventional system. This phenomenon takes place due to a very high coke oxidation rate in presence of CO_2 rather than H_2O.

Fig. 7 displays gas temperature profiles along the reactor for both systems. It is noticeable that in the first section of the reactor both models could predict the same profile for gas temperature due to the fact that concentration of coke precursors are quite

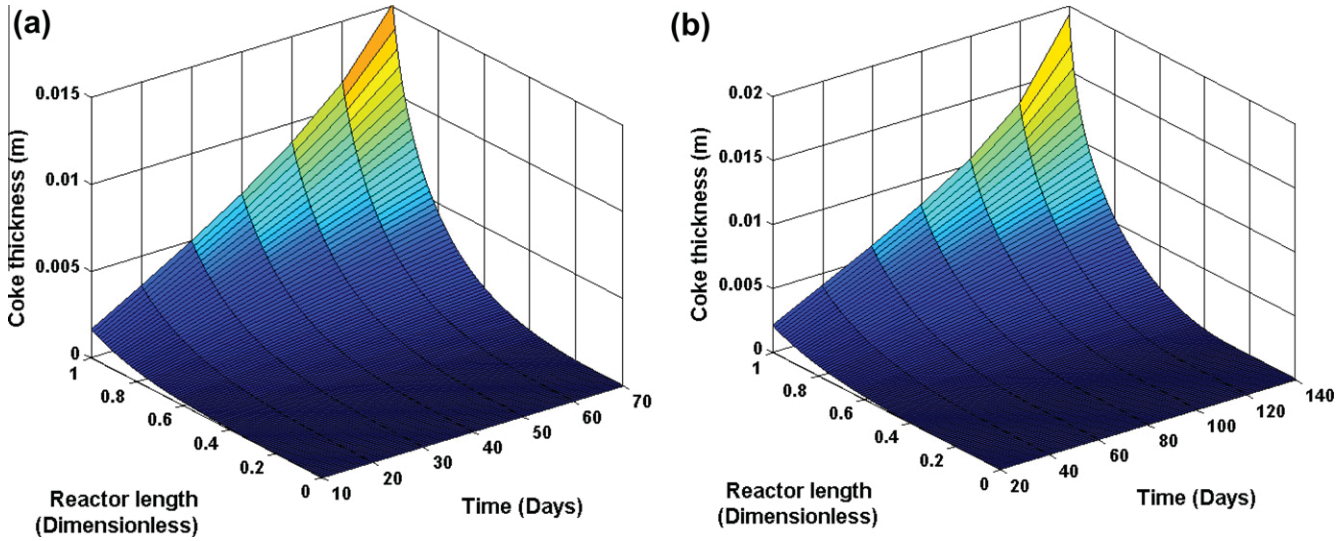

Fig. 9. The coke thickness along the length of cracking coils during a time period (a) in presence of steam and (b) in presence of CO_2.

low in this section and so the coke formation does not happen. However, coke formation begins by increasing the gas temperature and coke precursors' concentrations. It is clear that the coke formation rate for both models is equal, but the oxidation rate of coke in presence of CO_2 is considerably higher than the one in presence of steam. Therefore, the coke thickness in this novel system is less than the conventional one. This phenomenon leads to higher heat transfer to the coils and so the gas temperature in presence of carbon dioxide stands above the gas temperature in presence of steam.

Fig. 8 shows tube wall temperature profile in the 30th day of plant operation. Obviously, this profile in presence of steam is above the one in presence of CO_2 throughout the reactor. This phenomenon occurs because in the new system coke formation is less than the conventional one and as a result less generated heat can be accumulated in the tube walls.

Industrial plant should be shut down when the coke thickness inside the reactor wall reaches 10–20% of the tube diameter. As it is shown in Fig. 9a, the cracking process in presence of steam can continue nearly 70 days and after this period the plant should be shut down for decoking procedure. Nevertheless, the operation time for the novel model will be more than 140 days (Fig. 9b). For this reason, the process can produce more ethylene with considerably less operating and maintenance costs.

The 3D plot of tube wall temperature as a function of the length of reactor and time is shown in Fig. 10. As it can be seen, the run length of the reactor in conventional thermal cracking process is 70 days and the tube wall temperature reaches to 1370 K which is slightly less than the maximum allowable tube wall temperature (1100 °C). On the other hand, the temperature of tube wall in presence of CO_2 reaches to the maximum allowable temperature just after 140 days.

Fig. 11 presents the experimental tube wall temperatures during a run length of reactor in Jam Petrochemical Company. It is clear that in the first days of operating time the tube wall temperatures are below 1220 K because of no coke deposited in this period. However, this quantity reaches more than 1280 K as the time progressed. According to this figure, tube wall temperature fluctu-

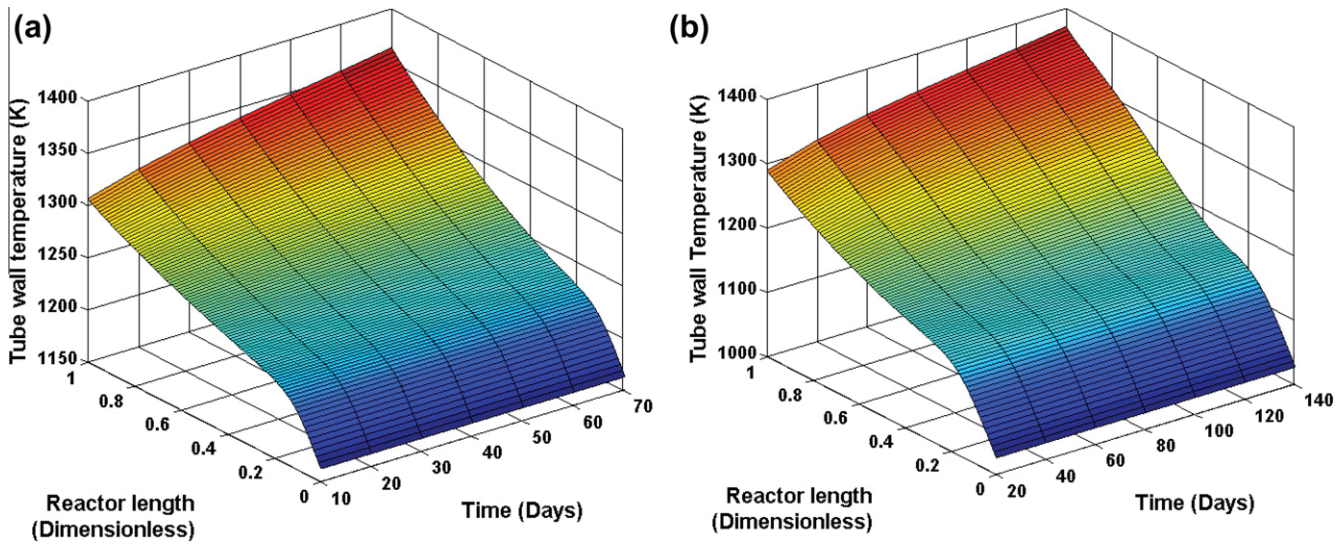

Fig. 10. The tube wall temperature along the length of cracking coils during a time period (a) in the presence of steam and (b) in the presence of CO_2.

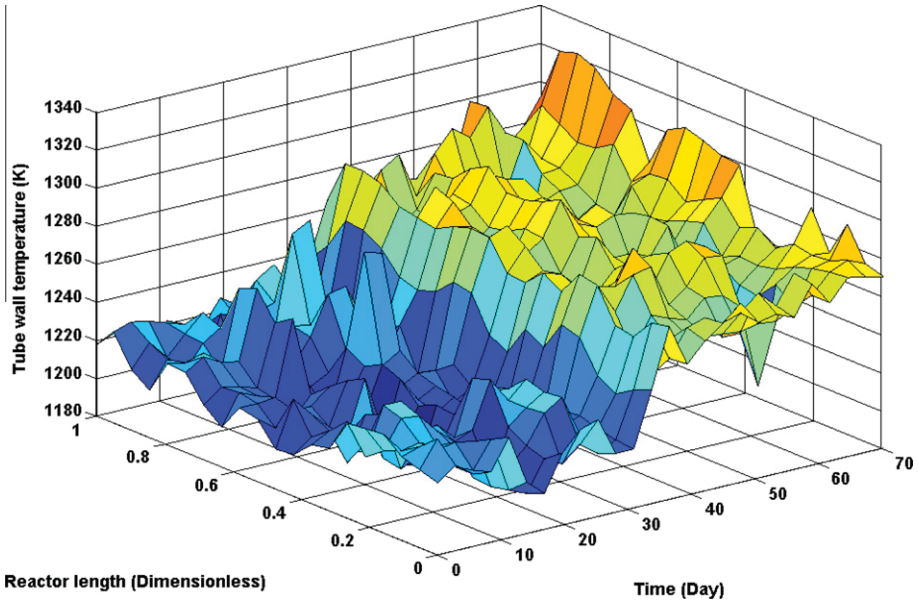

Fig. 11. The tube wall temperature along the length of cracking coils during a run length of reactor in 10th olefin.

ated widely as a function of reactor length and time. This is because the coke formation rate is different in various parts of cracking coils and so the heat transfer is not uniform along the reactor.

8. Conclusions

In this study, a gas thermal cracking process in domestic petrochemical company was simulated accurately. This company uses ethane for its gas pyrolysis process and produces some useful chemicals such as ethylene and hydrogen, which are the most important ones. First of all, a quasi-steady-state one dimensional model has been used to investigate thermal cracking process of ethane in presence of steam. A comparison between modeling results and industrial data from domestic petrochemical company shows an acceptable agreement. After that, the confirmed model was run in presence of carbon dioxide to investigate its effects on reactor operation and product yields. Some important parameters such as ethylene and hydrogen flow rates, gas temperature profile, tube wall temperature and coke thickness are compared in both cases. According to this comparison, the advantages of using CO_2 instead of steam in ethane thermal cracking are summarized as follows:

- The ethylene and hydrogen production yields increase noticeably in presence of CO_2.
- The run length of reactor in presence of CO_2 is twice as much as the one in presence of steam.
- The coke thickness in proposed system is considerably less than the conventional process.

References

[1] A. Campen, K. Mondal, T. Wiltowski, Separation of hydrogen from syngas using a regenerative system, Int. J. Hydrogen Energy 33 (2008) 332–339.
[2] M. Balat, Potential importance of hydrogen as a future solution to environmental and transportation problems, Int. J. Hydrogen Energy 33 (2008) 4013–4029.
[3] J. Gómez, J. Fierro, New catalytic routes for syngas and hydrogen production, Appl. Catal., A 144 (1996) 7–57.
[4] M. Rahimpour, R. Vakili, E. Pourazadi, A. Bahmanpour, D. Iranshahi, Enhancement of hydrogen production via coupling of MCH dehydrogenation reaction and methanol synthesis process by using thermally coupled heat exchanger reactor, Int. J. Hydrogen Energy (2011).
[5] F. Díaz Alvarado, F. Gracia, Steam reforming of ethanol for hydrogen production: thermodynamic analysis including different carbon deposits representation, Chem. Eng. J. 165 (2010) 649–657.
[6] T. Davidian, N. Guilhaume, E. Iojoiu, H. Provendier, C. Mirodatos, Hydrogen production from crude pyrolysis oil by a sequential catalytic process, Appl. Catal. B 73 (2007) 116–127.
[7] L. Basini, S. Cimino, A. Guarinoni, G. Russo, V. Arca, Olefins via catalytic partial oxidation of light alkanes over Pt/$LaMnO_3$ monoliths, Chem. Eng. J. 207–208 (2012) 473–480.
[8] M. Masoumi, M. Shahrokhi, M. Sadrameli, J. Tpwfighi, Modeling and control of a naphtha thermal cracking pilot plant, American Chemical Society, Washington, DC, 2006. ETATS-UNIS.
[9] A. Tarafder, B.C.S. Lee, A.K. Ray, G.P. Rangaiah, Multiobjective optimization of an industrial ethylene reactor using a nondominated sorting genetic algorithm, American Chemical Society, Washington, DC, 2005. ETATS-UNIS.
[10] K.Y. Grace Chan, F. Inal, S. Senkan, Suppression of coke formation in the steam cracking of alkanes: ethane and propane, Ind. Eng. Chem. Res. 37 (1998) 901–907.
[11] A.K.K. Lee, A.M. Aitani, Saudi ethylene plants move toward more feed flexibility, Oil Gas J. (1990) 60–65. Medium: X; Size.
[12] K. Keyvanloo, M. Sedighi, J. Towfighi, Genetic algorithm model development for prediction of main products in thermal cracking of naphtha: comparison with kinetic modeling, Chem. Eng. J. 209 (2012) 255–262.
[13] K. Keyvanloo, J. Towfighi, S.M. Sadrameli, A. Mohamadalizadeh, Investigating the effect of key factors, their interactions and optimization of naphtha steam cracking by statistical design of experiments, J. Anal. Appl. Pyrolysis 87 (2010) 224–230.
[14] Z. Belohlav, P. Zamostny, T. Herink, The kinetic model of thermal cracking for olefins production, Chem. Eng. Process. 42 (2003) 461–473.
[15] M.L. Poutsma, Fundamental reactions of free radicals relevant to pyrolysis reactions, J. Anal. Appl. Pyrolysis 54 (2000) 5–35.
[16] K.M. Sundaram, G.F. Froment, Modeling of thermal cracking kinetics. 3. Radical mechanisms for the pyrolysis of simple paraffins, olefins, and their mixtures, Ind. Eng. Chem. Fund. 17 (1978) 174–182.
[17] H. Ghassabzadeh, J. Towfighi Darian, P. Zaheri, Experimental study and kinetic modeling of kerosene thermal cracking, J. Anal. Appl. Pyrolysis 86 (2009) 221–232.
[18] D. Depeyre, C. Flicoteaux, F. Arbabzadeh, A. Zabaniotou, Modeling of thermal steam cracking of an atmospheric gas oil, Ind. Eng. Chem. Res. 28 (1989) 967–976.
[19] J. Towfighi, A. Niaei, R. Karimzadeh, G. Saedi, Systematics and modelling representations of LPG thermal cracking for olefin production, Korean J. Chem. Eng. 23 (2006) 8–16.
[20] S. Abghari, J. Darian, R. Karimzadeh, M. Omidkhah, Determination of yield distribution in olefin production by thermal cracking of atmospheric gas oil, Korean J. Chem. Eng. 25 (2008) 681–692.
[21] M. Sedighi, K. Keyvanloo, J. Towfighi, Modeling of thermal cracking of heavy liquid hydrocarbon: application of kinetic modeling, artificial neural

network, and neuro-fuzzy models, Ind. Eng. Chem. Res. 50 (2011) 1536–1547.
[22] K.M. Sundaram, G.F. Froment, Kinetics of coke deposition in the thermal cracking of propane, Chem. Eng. Sci. 34 (1979) 635–644.
[23] P.M. Plehiers, G.C. Reyniers, G.F. Froment, Simulation of the run length of an ethane cracking furnace, Ind. Eng. Chem. Proc. Des. Dev. 29 (1990) 636–641.
[24] J. Towfighi, J. Modarres, M. Omidkhah, Estimation of kinetic parameters of coking reaction rate in pyrolysis of naphtha, Int. J. Eng. Trans. B 17 (2004) 319–332.
[25] D. Salari, A. Niaei, J. Towfighi, P. Nakhostin Panahi, Coke inhibition during naphtha pyrolysis, Iran J. Chem. Eng. 6 (2009) 12–22.
[26] P.S. Virk, L.E. Chambers, H.N. Woebcke, Thermal hydrogasification of aromatic compounds, in: Coal Gasification, American Chemical Society, 1974, pp. 237–258.
[27] G.F. Froment, Coke formation in the thermal cracking of hydrocarbons, Rev. Chem. Eng. 64 (1990) 293–328.
[28] L.F. Albright, C.F. McConnell, K. Welther, Types of coke formed during the pyrolysis of light hydrocarbons, (1978).
[29] P. Kumar, D. Kunzru, Modeling of naphtha pyrolysis, Ind. Eng. Chem. Proc. Des. Dev. 24 (1985) 774–782.
[30] P. Kumar, D. Kunzru, Kinetics of coke deposition in naphtha pyrolysis, Can. J. Chem. Eng. 63 (1985) 598–604.
[31] R. Zou, Q. Lou, S. Mo, S. Feng, Study on a kinetic model of atmospheric gas oil pyrolysis and coke deposition, Ind. Eng. Chem. Res. 32 (1993) 843–847.
[32] M.R. Rahimpour, O. Dehghani, M.R. Gholipour, M.S. Shokrollahi Yancheshmeh, S. Seifzadeh Haghighi, A. Shariati, A novel configuration for Pd/Ag/α-Al_2O_3 catalyst regeneration in the acetylene hydrogenation reactor of a multi feed cracker, Chem. Eng. J. 198–199 (2012) 491–502.
[33] C. Riverol, M.V. Pilipovik, Optimization of the pyrolysis of ethane using fuzzy programming, Chem. Eng. J. 133 (2007) 133–137.
[34] V.R. Choudhary, K.C. Mondal, S.R. Mulla, Non-catalytic pyrolysis of ethane to ethylene in the presence of CO_2 with or without limited O_2, J. Chem. Sci. 118 (2006) 261–267.
[35] K.M. Sundaram, G.F. Froment, Modeling of thermal cracking kinetics – I: thermal cracking of ethane, propane and their mixtures, Chem. Eng. Sci. 32 (1977) 601–608.